



## RESEARCH ARTICLE

# Metabolic profiling of colorectal cancer organoids: A comparison between high-resolution magic angle spinning magnetic resonance spectroscopy and solution nuclear magnetic resonance spectroscopy of polar extracts

Wybe J. M. van der Kemp<sup>1</sup> | Maria T. Grinde<sup>2,3</sup> | Jon O. Malvik<sup>2</sup> |  
Hanneke W. M. van Laarhoven<sup>4</sup> | Jeanine J. Prompers<sup>1</sup>  | Dennis W. J. Klomp<sup>1</sup> |  
Boudewijn Burgering<sup>5</sup> | Tone Frost Bathen<sup>2</sup>  | Siver Andreas Moestue<sup>6,7</sup>

<sup>1</sup>Division of Imaging and Oncology, University Medical Centre (UMC) Utrecht, Utrecht, The Netherlands

<sup>2</sup>Department of Circulation and Medical Imaging, NTNU – Norwegian University of Science and Technology, Trondheim, Norway

<sup>3</sup>Department of Radiology and Nuclear Medicine, St. Olavs Hospital, Trondheim University Hospital, Trondheim, Norway

<sup>4</sup>Department of Medical Oncology, Cancer Center Amsterdam, Amsterdam University Medical Centers, University of Amsterdam, Amsterdam, The Netherlands

<sup>5</sup>Center for Molecular Medicine, Molecular Cancer Research, University Medical Center Utrecht, Utrecht, The Netherlands

<sup>6</sup>Department of Clinical and Molecular Medicine, NTNU – Norwegian University of Science and Technology, Trondheim, Norway

<sup>7</sup>Department of Pharmacy, Nord University, Bodø, Norway

## Correspondence

Wybe J. M. van der Kemp, Division of Imaging and Oncology, University Medical Centre (UMC) Utrecht, Utrecht, The Netherlands.  
Email: [w.j.m.vanderkemp@umcutrecht.nl](mailto:w.j.m.vanderkemp@umcutrecht.nl)

## Funding information

Research reported in this publication was funded by EU Horizon 2020, FETOPEN 2016–2017 Grant number: 801075; NICI. Experiments at the 600 MHz instrument for

## Abstract

Patient-derived cancer cells cultured in vitro are a cornerstone of cancer metabolism research. More recently, the introduction of organoids has provided the research community with a more versatile model system. Physiological structure and organization of the cell source tissue are maintained in organoids, representing a closer link to in vivo tumor models. High-resolution magic angle spinning magnetic resonance spectroscopy (HR MAS MRS) is a commonly applied analytical approach for metabolic profiling of intact tissue, but its use has not been reported for organoids. The aim of the current work was to compare the performance of HR MAS MRS and extraction-based nuclear magnetic resonance (NMR) in metabolic profiling of wild-type and tumor progression organoids (TPOs) from human colon cancer, and further to investigate how the sequentially increased genetic alterations of the TPOs affect the metabolic profile. Sixteen metabolites were reliably identified and quantified both in spectra based on NMR of extracts and HR MAS MRS of intact organoids. The metabolite concentrations from the two approaches were highly correlated ( $r = 0.94$ ), and both approaches were able to capture the systematic changes in metabolic features introduced by the genetic alterations characteristic of colorectal cancer progression (e.g., increased levels of lactate and decreased levels of myo-inositol and phosphocholine with an increasing number of mutations). The current work highlights that HR MAS MRS is a well-suited method for metabolic profiling of intact organoids, with the additional benefit that the nondestructive nature of HR MAS enables subsequent recovery of the organoids for further analyses based on nucleic acids or proteins.

**Abbreviations used:** Ala, alanine; Cho, choline; GABA, gamma-aminobutyric acid; Gln, glutamine; Glu, glutamate; Gly, glycine; GPC, glycerophosphocholine; GSH, glutathione; HR MAS MRS, high-resolution magic angle spinning magnetic resonance spectroscopy; Iso, isoleucine; Lac, lactate; Leu, leucine; Myo-In, myo-inositol; PC, phosphocholine; PCA, principal component analysis; PE, phosphoethanolamine; Pro, proline; TPO, tumor progression organoid; Val, valine.

Wybe J. M. van der Kemp and Maria T. Grinde shared authorship.

This is an open access article under the terms of the [Creative Commons Attribution](https://creativecommons.org/licenses/by/4.0/) License, which permits use, distribution and reproduction in any medium, provided the original work is properly cited.

© 2022 The Authors. *NMR in Biomedicine* published by John Wiley & Sons Ltd.

solution NMR were supported by uNMR-NL, the National Roadmap Large-Scale NMR Facility of the Netherlands (NWO grant 184.032.207). The HRMAS MRS analyses were performed at the MR Core Facility, Norwegian University of Science and Technology (NTNU). MR core facility is funded by the Faculty of Medicine at NTNU and Central Norway Regional Health Authority.

#### KEYWORDS

colorectal cancer, HR MAS MRS, lactate, myo-inositol, NMR, organoids, phosphocholine, tumor progression organoids

## 1 | INTRODUCTION

For decades, patient-derived cancer cells cultured *in vitro* have been a cornerstone of mechanistic cancer research. This approach has led us to the point where we have mapped multiple metabolic pathways that are dysregulated in cancer, and several drugs targeting key metabolic enzymes have been evaluated in clinical trials.<sup>1–4</sup>

Although this model system has led to major breakthroughs in our understanding of cancer, it also has significant limitations. It is clear that the metabolic characteristics of cancer cells cultured *in vitro* differ from those observed *in vivo*. Mori et al.<sup>5</sup> demonstrated this elegantly by comparing the choline (Cho) metabolic pathway in MDA-MB-231 cells when cultured *in vitro* and as xenograft tumors, respectively. Moreover, the cells are frequently selected based on their ability to survive and proliferate as monocultures under conditions that do not successfully mimic the tumor microenvironment. Spatial orientation, differentiation, and interaction between different cell types are examples of aspects that are important in cancer, but which are not easily studied in classical cell cultures.<sup>6,7</sup>

In recent years, the art of generating three-dimensional (3D), multicell masses known as “organoids” has evolved.<sup>8</sup> Organoids can be established from stem-like cells, and while they are able to self-proliferate, they also maintain the physiological structure and organization of their source tissue. In many aspects, organoids represent a bridge between *in vitro* monoculture and *in vivo* tumor models, and they have therefore attracted significant interest in several fields of cancer research. While not presenting the full complexity of a tumor in a living organism, the heterogeneity of cancer cells and the impact of stromal components on regulation of metabolic function are maintained.<sup>7</sup>

For metabolic profiling, methods based on mass spectrometry have been developed. However, mass spectrometry requires extensive sample preparation and calibration curves for individual metabolites, and magnetic resonance (MR)-based analysis is an attractive alternative, being a quantitative method with high reproducibility, with relatively easy sample preparation and potential for clinical translation of metabolic biomarkers. In particular, high-resolution magic angle spinning MR spectroscopy (HR MAS MRS) has proven to be a useful tool in translational cancer metabolomics, because of its ability to extract metabolic information from intact tissues in a nondestructive manner.<sup>9</sup> However, application of HR MAS MRS to cancer organoids has not yet been reported. In this study, we compare the performance of HR MAS MRS and extraction-based nuclear magnetic resonance (NMR) for metabolic profiling of human intestinal stem cell-derived organoids, representing the sequential acquisition of genetic alterations in colorectal cancer.<sup>10</sup> Both the analytical correlation between the two methods and their ability to detect metabolic differences between organoids are reported.

## 2 | METHODS

### 2.1 | Organoid culturing

Wild-type (WT) and tumor progression organoids (TPOs) from human colon were obtained from the organoid biobank (HUB Organoids, Utrecht, The Netherlands). The TPOs were established as described by Drost et al.<sup>10</sup> and consisted of the following types: TPO0 (WT), TPO2 (APC-KRAS mutated), TPO2 (APC-P53 mutated), TPO3 (APC-KRAS-p53 mutated), and TPO4 (APC-KRAS-p53-SMAD4 mutated). Organoids were cultured in small droplets (~20  $\mu$ l) of Matrigel in well plates with six wells containing 200  $\mu$ l of Matrigel per well and 2 ml of expansion medium. The composition of the expansion medium for each type of organoid is shown in Table 1.

Organoids were plated, after trypsinizing as multiple cell fragments. Rho-associated protein kinase (ROCK) inhibitor Y-27632 (10  $\mu$ M) was added to the medium for the first 5 days to enhance stem cell survival after trypsinization.<sup>11</sup> After culturing for 5 days on expansion medium, the organoids were re-plated less dense and cultured for 5 days on differentiation medium. The differentiation medium composition is shown in Table 2.

The medium of the organoids was refreshed every 48 h and also 24 h before harvesting, the latter to reduce the effect of medium depletion on the organoid metabolome as measured by <sup>1</sup>H NMR. To investigate the possible influence of culturing duration on metabolite concentrations, the organoids were harvested at three different time points: after 10 days of total culturing time (the 0-h samples), 12 days (the 48-h samples),

**TABLE 1** Composition of expansion medium (10.33 ml) for colon TPO culturing

	+++	Wnt	R-spondin	Noggin	B27	n-AC	Nicotinamide	EGF	A83	SB
WT	2 ml	5 ml	2 ml	1 ml	200 $\mu$ l	25 $\mu$ l	100 $\mu$ l	1 $\mu$ l	1 $\mu$ l	3.3 $\mu$ l
APC-KRAS	9 ml	–	–	1 ml	200 $\mu$ l	25 $\mu$ l	100 $\mu$ l	–	1 $\mu$ l	3.3 $\mu$ l
APC-P53	9 ml	–	–	1 ml	200 $\mu$ l	25 $\mu$ l	100 $\mu$ l	1 $\mu$ l	1 $\mu$ l	3.3 $\mu$ l
APC-KRAS-P53	9 ml	–	–	1 ml	200 $\mu$ l	25 $\mu$ l	100 $\mu$ l	–	1 $\mu$ l	3.3 $\mu$ l
APC-KRAS-P53-SMAD4	10 ml	–	–	–	200 $\mu$ l	25 $\mu$ l	100 $\mu$ l	–	1 $\mu$ l	3.3 $\mu$ l

Abbreviations: TPO, tumor progression organoid; WT, wild-type.

+++ : 500 ml of DMEM/F-12 + 5 ml of penicilline streptomycine + 5 ml of HEPES buffer + 5 ml of Glutamax 100x; B27 Thermofischer (50x); n-AC: n-acetyl-cysteine 500 mM; nicotinamide 1000 mM; EGF: 50  $\mu$ g/ml human epithelial growth factor; A83: 0.5 mM; SB: 9.1 mM SB20219.

**TABLE 2** Composition of differentiation medium (10.20 ml) for colon TPO culturing

	+++	Wnt	R-spondin	Noggin	B27	EGF	A83
WT	5.5 ml	2.5 ml	1 ml	1 ml	200 $\mu$ l	1 $\mu$ l	1 $\mu$ l
APC-KRAS	9 ml	–	–	1 ml	200 $\mu$ l	–	1 $\mu$ l
APC-P53	9 ml	–	–	1 ml	200 $\mu$ l	1 $\mu$ l	1 $\mu$ l
APC-KRAS-P53	9 ml	–	–	1 ml	200 $\mu$ l	–	1 $\mu$ l
APC-KRAS-P53-SMAD4	10 ml	–	–	–	200 $\mu$ l	–	1 $\mu$ l

Abbreviations: TPO, tumor progression organoid; WT, wild-type.

+++ : 500 ml of DMEM/F-12 + 5 ml of penicillin streptomycin + 5 ml of HEPES buffer + 5 ml of Glutamax 100x; B27 Thermofischer (50x); n-AC: n-acetyl-cysteine 500 mM; EGF: 50  $\mu$ g/ml human epithelial growth factor; A83: 0.5 mM.

and 14 days (the 96-h samples). Just prior to organoid harvesting, a digital image at 40 x magnification of each well was created with a Nikon TS 100 microscope.

Organoid harvesting was performed on ice. The medium solution was pipetted off and the wells were carefully rinsed with 1 ml of ice-cold saline without disrupting the Matrigel. The rinsing saline was pipetted off and replaced with 2 ml of ice-cold saline and the Matrigel with the organoids was disrupted by pipetting fiercely up and down. The ice-cold saline with the disrupted Matrigel and organoids were gathered in 15-ml falcon tubes and the wells were rinsed once more with 1 ml of ice-cold saline. Next, 9 ml of ice-cold saline was added to the 3 ml of ice-cold saline with disrupted Matrigel and organoids in the falcon tubes, and the tubes were centrifuged at 0°C at 264 g for 4 min. The supernatant was carefully pipetted off. To dilute the medium solution residue below the <sup>1</sup>H NMR detection limit, the obtained organoid pellet was resuspended in 10 ml of ice-cold normal saline three times. After the washing step, the organoid pellets were snap-frozen in falcon tubes with liquid nitrogen and stored at –80°C until HR MAS MRS analysis. Samples for HR MAS were shipped on dry ice to Trondheim. To the pellet samples that were destined for extraction NMR, 800  $\mu$ l of ice-cold absolute methanol was added prior to snap-freezing. All organoids destined for extraction NMR were cultured and extracted in duplicate, providing full biological replicates. To reduce the number of samples, 48-h extraction samples were not prepared for all organoid lines.

## 2.2 | Extraction

Glass beads (~ twice the volume of the organoid pellet) were added to the organoid pellet in 800  $\mu$ l of absolute methanol and the samples were sonicated on ice (0°C) (two x 45 s) with a rod sonicator. After sonication, 800  $\mu$ l of ice-cold chloroform was added and the samples were vortexed (five x 30 s) intermittently and stored on ice. Subsequently, 800  $\mu$ l of ice-cold milliQ water was added and the samples were vortexed (five x 30 s) intermittently and stored on ice. The tubes were centrifuged at 0°C for 20 min at 4200 g, to obtain phase separation and a thin protein layer between the aqueous methanolic phase and the chloroform phase. Approximately 1.2 ml of the methanolic water fractions, with the polar metabolites, were pipetted off and dried in a speedvac for 2 h. Additionally, 300  $\mu$ l of ice-cold methanol was added to the pellet samples and vortexed (three x 30 s) intermittently and subsequently 300  $\mu$ l of milliQ water was added and the samples were vortexed (three x 30 s) intermittently. The samples were centrifuged again (at 0°C) for 20 min at 4200 g and the water methanolic fractions were pipetted off and added to the corresponding fractions in the speedvac. The dried organoid extract samples were stored at –80°C until NMR measurement.

Prior to NMR measurement, the frozen dried samples were dissolved in 550  $\mu\text{l}$  of 50 mM phosphate buffer (pH 7.3) with 0.027 mM trimethylsilylpropanoic acid (TSP) as the reference compound and 10%  $\text{D}_2\text{O}$  for locking. The samples were centrifuged for 4 min and 500  $\mu\text{l}$  of the solution was pipetted into an NMR tube.

## 2.3 | NMR from extracts

The NMR measurements were performed on a Bruker Avance 600-MHz ultra (Bruker Biospin GmbH, Germany) using a gradient-pulsed one-dimensional (1D) Nuclear Overhauser Enhancement Spectroscopy (NOESY) sequence (noesygppr1d) with an acquisition time of 4 s; 57,690 datapoints; 1s presaturation delay time; sample averaging was varied between 256 to 784, to obtain sufficient signal to noise for later spectral fitting. The temperature was kept at 25°C during the whole experiment. The FIDs were multiplied with an exponential line broadening of 0.5 Hz and Fourier-transformed into 128 k.

## 2.4 | HR MAS MRS acquisition

Organoid samples were thawed and put into 20- $\mu\text{l}$  disposable inserts. Lock reference ( $\sim 4.3$  mg/ $\sim 4$   $\mu\text{l}$ ) containing  $\text{D}_2\text{O}$  with formate (25 mM) was added to the samples. The inserts were then inserted into 80- $\mu\text{l}$  zirconium HR MAS rotors (4-mm diameter) and sealed. The HR MAS MR spectra were recorded using a Bruker Avance III spectrometer (14.1 T) containing a  $^1\text{H}/^{13}\text{C}$  MAS probe. The samples were spun at 5 kHz at magic angle, and the temperature was kept at 5°C during the whole experiment. MR spectra were acquired using the following MR sequence and acquisition parameters: a 1D  $^1\text{H}$  NOESY pulse sequence with water presaturation (Bruker; noesygppr1d); the acquisition time was 2.7 s; the presaturation delay time was 1 s; the acquisition bandwidth was 29.9 ppm; there were 98,304 datapoints; and 256 scans were acquired for all spectra. The FIDs were multiplied with an exponential line broadening of 0.3 Hz and Fourier-transformed into 64 k.

The acquisition of HR MAS NOESY spectra was chosen rather than a Carr–Purcell–Meiboom–Gill (CPMG) method, because it also shows lipids and/or other macromolecules in the samples that may change with mutation status.

## 2.5 | Analysis of MR spectra from extracts and HR MAS

After MR acquisition, each spectrum was manually preprocessed in Topspin (v. 4.0.6). This included referencing of the spectra using alanine [Ala] at 1.48 ppm as an internal standard, and zero and first order phasing. Selected metabolites (phosphocholine [PC], lactate [Lac], myo-inositol [Myo-In], phosphoethanolamine [PE], glycerophosphocholine [GPC], Ala, glutathione [GSH], glutamate [Glu], glutamine [Gln], glycine [Gly], choline [Cho], gamma-aminobutyric acid [GABA], proline [Pro], valine [Val], isoleucine [Iso], and leucine [Leu]) in the MR spectra were spectrally fitted manually using a Chenomx profiler. Prior to quantification in the Chenomx profiler, all the extraction NMR spectra were apodized to a final linewidth of 1.1 Hz, based on the linewidth of the internal standard TSP. The formate peak was used for the HR MAS spectra.

Fitting individual peaks on top of broad peaks in the HR MAS spectra was performed by subtracting fit from spectrum to look for any remaining sharp peaks, or by approximately measuring the heights of the fitted peaks compared with the spectrum. Quantified metabolite concentrations were then found, and each concentration was normalized to the total amount of all metabolite concentrations (relative metabolite concentration =  $\frac{[\text{Metabolite}]}{\sum [\text{All metabolites}]}$ ). The relative metabolite concentrations from corresponding HR MAS and extract MR spectra were then matched, and the linear association between the metabolite levels obtained was measured by calculating Pearson correlation coefficients. One sample was removed from the analysis attributable to outlying characteristics (TPO2, APC-p53, 0 h). One other MR spectrum was missing from the extracts (TPO2, APC-p53, 48 h).

The normalized metabolite concentrations were then imported into MATLAB (v. R2017a). PLS toolbox (Eigenvector Research, v. 8.1.1) was used for principal component analysis (PCA). Metabolite concentrations were preprocessed using mean centering before the analysis. PCA score plots and loading profiles from PCA were then investigated.

HR MAS MR spectra were also analyzed using PCA to exploit additional information from other spectral components than the quantified metabolites. The spectra were then imported into MATLAB (v. R2017a), aligned using the max peak value from formate at 8.45 ppm, baseline corrected using asymmetric least squares baseline estimation as described,<sup>12</sup> and peak aligned using icoshift.<sup>13</sup> The spectral area from 8.7 to 0.8 ppm was selected for multivariate analysis. The residual water and formate peaks, and regions without visible peaks or contamination (ethanol and methanol), were removed before analysis (i.e., 8.47–8.43, 5.4–4.5, 3.47–3.436, 3.133–3.06, 2.81–2.658, and 1.18–1.04 ppm). Spectra were mean normalized and mean centered before PCA, which was performed using PLS toolbox. PC1 and PC2 score plots and loading profiles from the HR MAS MR spectra were visually inspected.

### 3 | RESULTS

Microscopic images (40 x magnification) of the different organoid cultures are shown in Figure 1. The WT organoids are predominantly cystic, while the cancerous TPOs become more solid-like as the number of mutations increases. Note that the TPO0 and TPO2 organoid cultures are of comparable organoid density, while the TPO3 and TPO4 organoids are plated more densely. As the organoids are cultured under static conditions (i.e., the medium is changed every 48 h, and also 24 h before harvesting), the organoid density is expected to influence not only the medium composition at harvesting, but also the metabolic profile of the organoids.

Samples from each TPO were analyzed using both  $^1\text{H}$  HR MAS MRS of thawed snap-frozen organoids and  $^1\text{H}$  NMR after polar phase metabolite extraction. We were able to reliably identify and quantify about 16 metabolites from the spectra. Representative NMR spectra from extracts and HR MAS MR spectra from intact organoids are shown in Figure 2. The main difference between the extract NMR spectra and the HR MAS MR spectra was the presence of lipids. Polar phase (methanol) metabolite extraction removes lipids from the samples and lipids are consequently

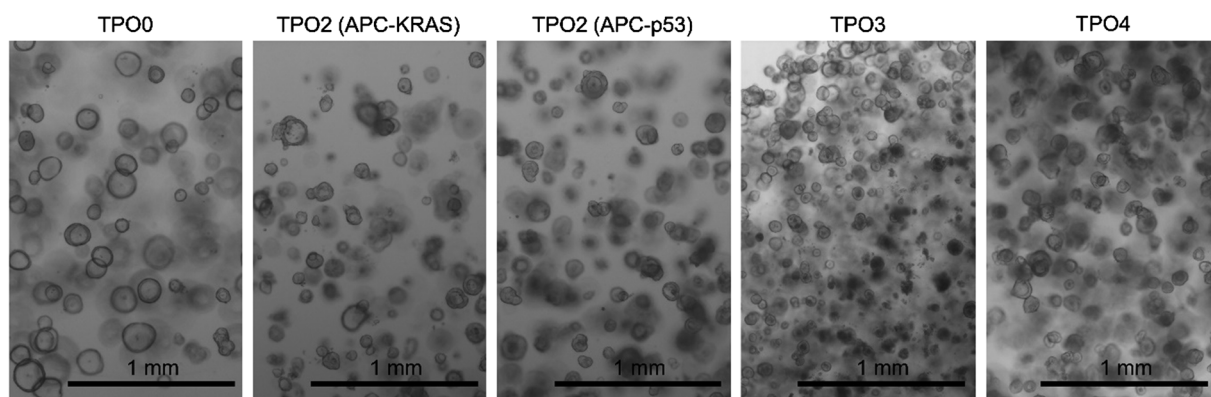


**FIGURE 1** Representative microscope images (at 40 x magnification) from each TPO, all captured at 0 h, that is, 10 days after trypsinizing with 5 days' growth on expansion medium and 5 days on differentiation medium. TPO, tumor progression organoid

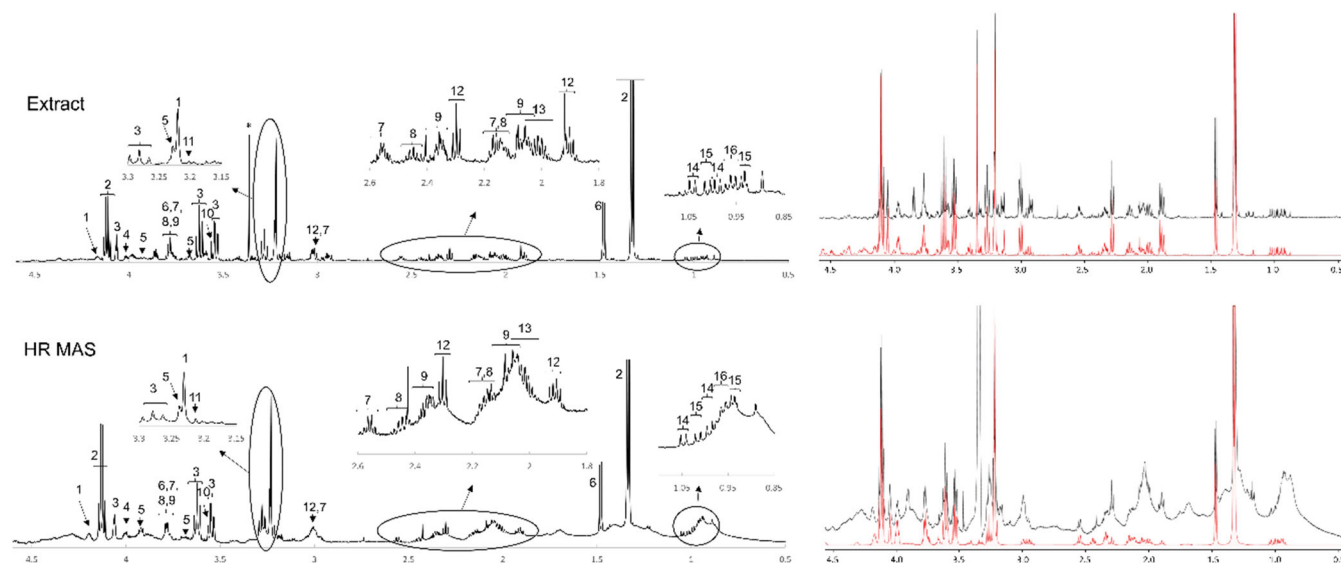


**FIGURE 2** Representative NMR spectra (TPO3, 0 h) from extract (top panel) and HR MAS  $^1\text{H}$  (bottom panel) MRS analysis. The labeled metabolites are: 1: PC, 2: Lac, 3: Myo-In, 4: PE, 5: GPC, 6: Ala, 7: GSH, 8: Gln, 9: Glu, 10: Gly, 11: Cho, 12: GABA, 13: Pro, 14: Val, 15: Iso, 16: Leu. \*Methanol contamination. Metabolites downfield ( $>4.7$  ppm) were difficult to reliably identify and quantify due to low SNR, and this part of the spectrum is thus not included in the figure. Ala, alanine; Cho, choline; GABA, gamma-aminobutyric acid; Gln, glutamine; Glu, glutamate; Gly, glycine; GPC, glycerophosphocholine; GSH, glutathione; HR MAS, high-resolution magic angle spinning; Iso, isoleucine; Lac, lactate; Leu, leucine; MRS, magnetic resonance spectroscopy; Myo-In, myo-inositol; NMR, nuclear magnetic resonance; PC, phosphocholine; PE, phosphoethanolamine; Pro, proline; SNR, signal-to-noise ratio; TPO, tumor progression organoid; Val, valine

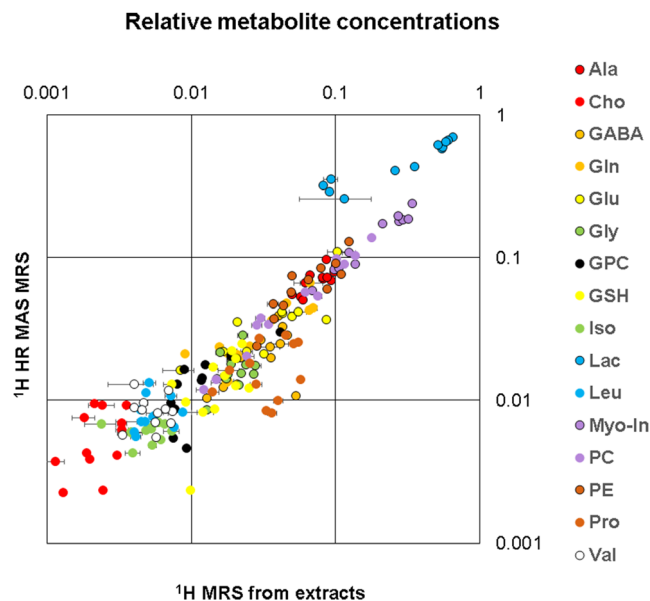


**FIGURE 3** Analysis of relative metabolite concentrations found in <sup>1</sup>H NMR spectra from extracts versus HR MAS MR spectra. Relative metabolite concentrations from HR MAS and extract <sup>1</sup>H NMR analysis;  $R = 0.94$ ,  $p < 0.0001$ . Each dot represents the relative concentration of one metabolite from one sample in the case of HR MAS and the average of two samples in the case of extracts. This means that the variation in concentration per metabolite shown depends on organoid type and organoid culturing time. Extracted samples are the average of full biological replicates with the tips of the horizontal bars representing the individual experimental values. In cases where no bars are visible, the experimental values coincide within the plotted symbol. Ala, alanine; Cho, choline; GABA, gamma-aminobutyric acid; Gln, glutamine; Glu, glutamate; Gly, glycine; GPC, glycerophosphocholine; GSH, glutathione; <sup>1</sup>H NMR, proton nuclear magnetic resonance; HR MAS MR, high-resolution magic angle spinning magnetic resonance; Iso, isoleucine; Lac, lactate; Leu, leucine; Myo-In, myo-inositol; PC, phosphocholine; PE, phosphoethanolamine; Pro, proline; Val, valine

**TABLE 3** Relative metabolite concentrations (mean  $\pm$  SD) from organoid extracts MRS and from HR MAS, the correlation between them and  $p$  values. Note that the relative metabolite concentrations are averages over all organoid lines and time points

Metabolite name	Mean $\pm$ SD Extracts	Mean $\pm$ SD HR MAS	Pearson correlation coeff. (r)	$p$ value
Ala	0.08 $\pm$ 0.02	0.07 $\pm$ 0.01	0.75	0.03*
Cho	0.023 $\pm$ 0.001	0.057 $\pm$ 0.003	0.44	0.80
GABA	0.03 $\pm$ 0.01	0.022 $\pm$ 0.009	0.49	0.0006*
Glu	0.04 $\pm$ 0.03	0.04 $\pm$ 0.03	0.80	0.03*
Gln	0.03 $\pm$ 0.02	0.03 $\pm$ 0.02	0.87	0.02*
GSH	0.016 $\pm$ 0.006	0.013 $\pm$ 0.006	0.58	0.08
Gly	0.020 $\pm$ 0.005	0.017 $\pm$ 0.005	0.34	0.2
GPC	0.014 $\pm$ 0.014	0.010 $\pm$ 0.007	0.87	0.02*
Iso	0.005 $\pm$ 0.001	0.0060 $\pm$ 0.0008	0.09	0.37
Lac	0.4 $\pm$ 0.2	0.5 $\pm$ 0.2	0.98	0.01*
Leu	0.006 $\pm$ 0.001	0.008 $\pm$ 0.002	0.14	0.35
Myo-In	0.2 $\pm$ 0.1	0.14 $\pm$ 0.06	0.97	0.01*
PC	0.07 $\pm$ 0.05	0.06 $\pm$ 0.04	0.98	0.009*
PE	0.06 $\pm$ 0.03	0.07 $\pm$ 0.03	0.87	0.02*
Pro	0.04 $\pm$ 0.01	0.018 $\pm$ 0.008	0.34	0.2
Val	0.006 $\pm$ 0.001	0.008 $\pm$ 0.002	-0.03	0.4

Abbreviations: Ala, alanine; Cho, choline; GABA, gamma-aminobutyric acid; Gln, glutamine; Glu, glutamate; Gly, glycine; GPC, glycerophosphocholine; GSH, glutathione; HR MAS, high-resolution magic angle spinning; Iso, isoleucine; Lac, lactate; Leu, leucine; MRS, magnetic resonance spectroscopy; Myo-In, myo-inositol; PC, phosphocholine; PE, phosphoethanolamine; Pro, proline; SD, standard deviation; Val, valine.

\* $p < 0.05$ .

only visible in the HR MAS MR NOESY spectra. Broad peaks from lipids can be suppressed by a CPMG T2 filter in the HR MAS MR spectra. However, lipid content may differ between TPOs and could be a potential biomarker for malignancy.

The relative metabolite concentrations obtained from the extract NMR and HR MAS MR spectra are shown in Figure 3. The metabolite concentrations of the extraction samples are averages of full biological duplicates, where the tips of the horizontal bars represent the original experimental values. Looking at all the metabolites, we observed that the concentrations were highly correlated ( $r = 0.94$ ,  $p < 0.0001$ ). The correlation coefficients and  $p$  values for individual metabolites are shown in Table 3. The relative concentration of each metabolite was analyzed using PCA, as shown in Figure 4. The analysis shows that PC1 explains 83.7% of the variance in relative metabolite concentration from the extract NMR spectra, and 94.6% from HR MAS MR spectra. TPO3 and TPO4 were characterized by lower levels of Myo-In, PC, Glu, and Gln, and higher levels of Lac. Analysis of HR MAS MR spectra by PCA confirmed that TPO0 and TPO2 had higher levels of Myo-In, PC, PE, Glu, and Gln, and lower levels of Lac, compared with TPO3 and TPO4. Adding pareto scaling before PCA gave very similar results (not shown). Figure 5 shows an overview of the relative concentration of Lac, Myo-In, Glu, Gln, Pc, and PE from the extracted organoid samples at two different time points. There appears to be no clearly distinguishable trend of relative metabolite concentration and culturing duration. The HR MAS MR spectra also contained signals from lipids. No clear differences in the amount of lipids were observed between different TPO types. Score and loading profiles from PCA of HR MAS MR spectra are shown in Figure 6.

## 4 | DISCUSSION

In this study we compared metabolite levels obtained by HR MAS MRS of thawed snap-frozen organoid pellets and solution NMR of polar organoid extracts. Both methods showed increased levels of Lac and decreased levels of Myo-In and PC with increased TPO state. The two

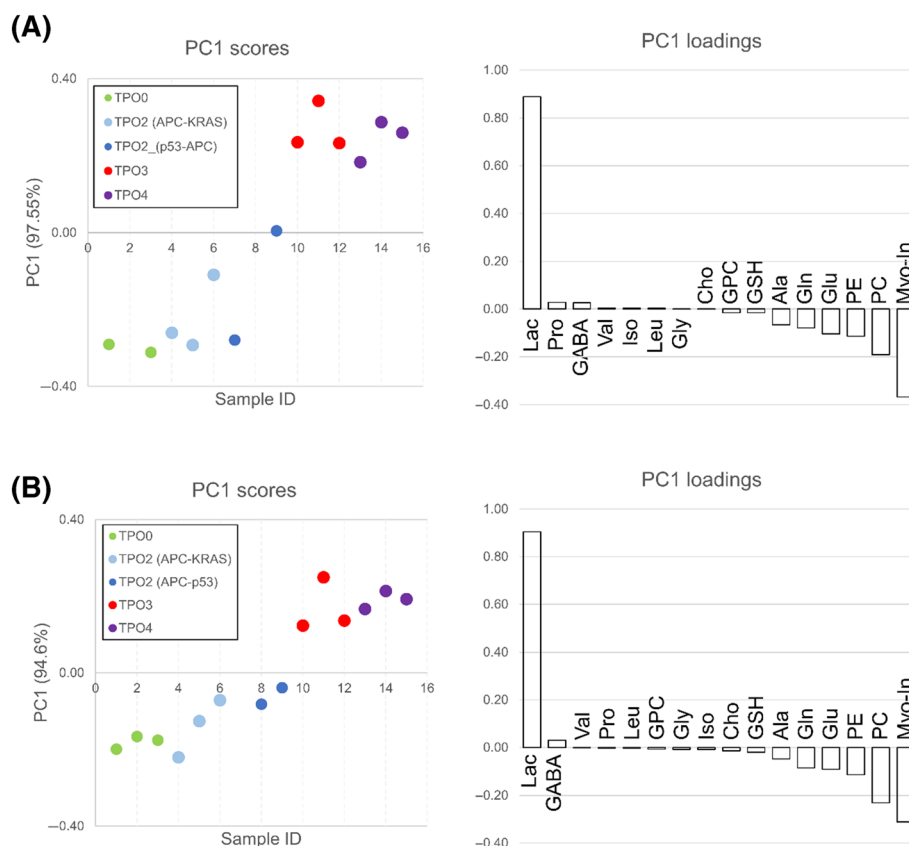


**FIGURE 4** PCA from metabolite concentrations in (A) <sup>1</sup>H MR spectra from extracts and (B) HR MAS analysis. PC1 scores for each sample (left panel) and corresponding loading profile (right panel). Sample ID: 1: TPO0\_0 h, 2: TPO0\_48 h, 3: TPO0\_96 h, 4: TPO2\_0 h, 5: TPO2\_48 h, 6: TPO2\_96 h, 7: TPO2\_p53APC\_0 h, 8: TPO2\_p53APC\_48 h, 9: TPO2\_p53APC\_96 h, 10: TPO3\_0 h, 11: TPO3\_48 h, 12: TPO3\_96 h, 13: TPO4\_0 h, 14: TPO4\_48 h, 15: TPO4\_96 h. Ala, alanine; Cho, choline; GABA, gamma-aminobutyric acid; Gln, glutamine; Glu, glutamate; Gly, glycine; GPC, glycerophosphocholine; GSH, glutathione; HR MAS, high-resolution magic angle spinning; Iso, isoleucine; Lac, lactate; Leu, leucine; Myo-In, myo-inositol; PC, phosphocholine; PCA, principal component analysis; PE, phosphoethanolamine; Pro, proline; TPO, tumor progression organoid; Val, valine

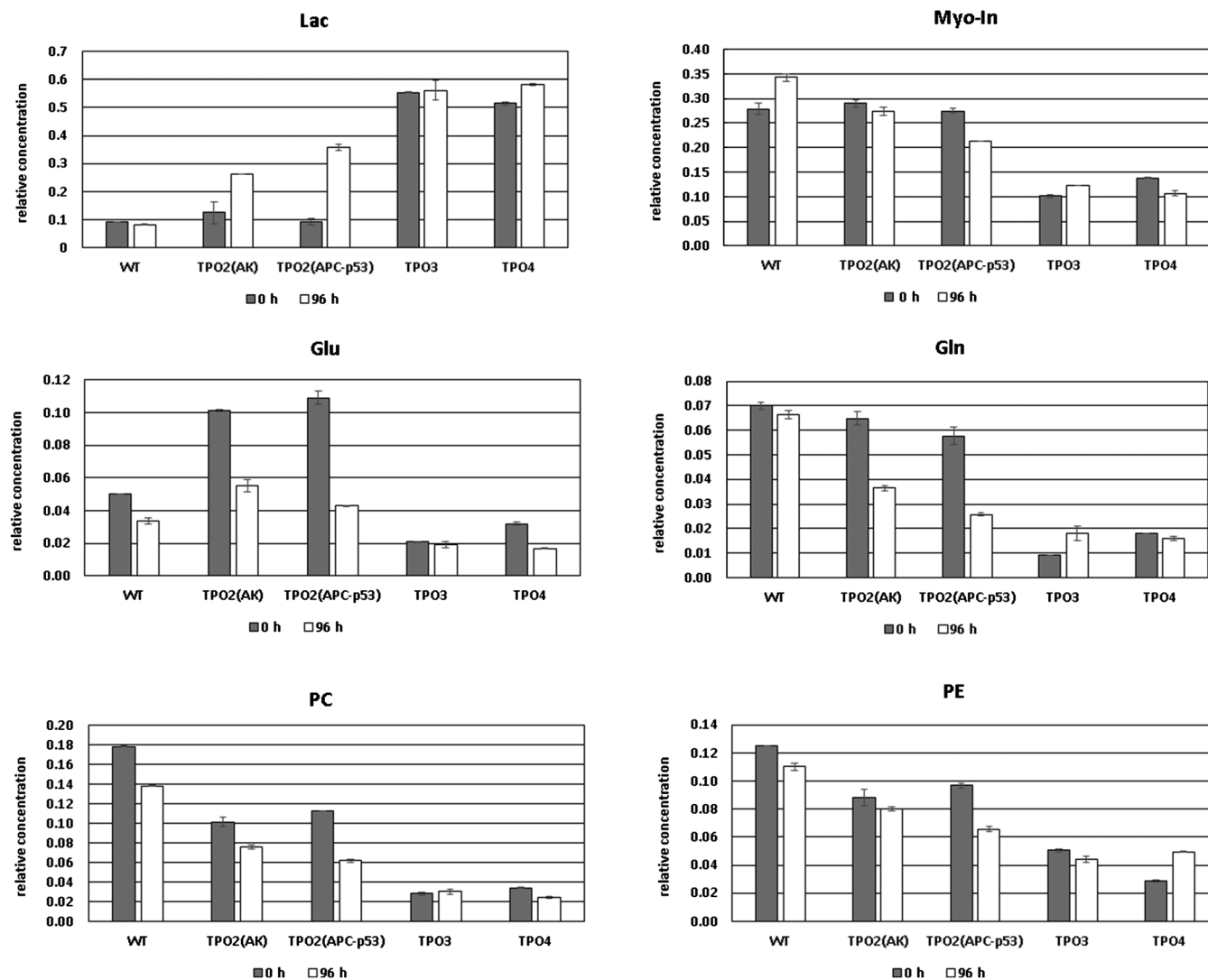


**FIGURE 5** Selection of relative metabolite concentrations measured in organoid extracts at 0 h (10 days' culturing) and 96 h (14 days' culturing) as a function of the number of mutations. Data shown are average values from full biological replicates with the individual experimental values shown by the tips of the "error" bars. Gln, glutamine; Glu, glutamate; Lac, lactate; Myo-In, myo-inositol; PC, phosphocholine; PE, phosphoethanolamine; TPO, tumor progression organoid; WT, wild-type

techniques led to similar results across 16 metabolites, indicating that HR MAS is a good method of choice as sample preparation is easy and straightforward compared with the extraction procedure.

For determination of low-molecular metabolites in cells and organoids using MRS, selecting the appropriate unit of measurement is not trivial. In extraction-based NMR, metabolite levels can, for example, be related to the number of cells, the dry weight of the cells, or the total amount of protein in the sample. Determining these variables adds to the analytical variability and may not necessarily add to the biological significance of the experiments. In metabolomics, it is therefore common practice to use multivariate statistical tools to compare cells that are cultured under different conditions or exposed to different interventions without the need for normalization to biomass.<sup>14</sup> While this relaxes the requirements for analytical accuracy, the precision must be sufficient to allow reproducible comparisons of specimens. The same applies to metabolic analysis of organoids. As MRS inherently is an analytical technique with high accuracy and precision,<sup>15,16</sup> metabolic profiling of organoids should be performed using methods that introduce as few sources of analytical error as possible. In this work, we therefore aimed to evaluate the functional performance of a method that includes as few preparatory steps as possible, and compare the results with those obtained with a classical extraction-based NMR protocol. As the sample preparation is fundamentally different, direct comparison of absolute concentrations is not relevant. Instead, we evaluated the overall congruence of the two datasets by means of Pearson correlation, and their ability to reveal metabolic differences between organoid lines by means of PCA.

In contrast to extraction NMR, the HR MAS MRS protocol provides information from intact organoids, and no loss of metabolites is expected during sample preparation. Although the presence of macromolecules could, in theory, cause restricted rotational tumbling of metabolites, visual



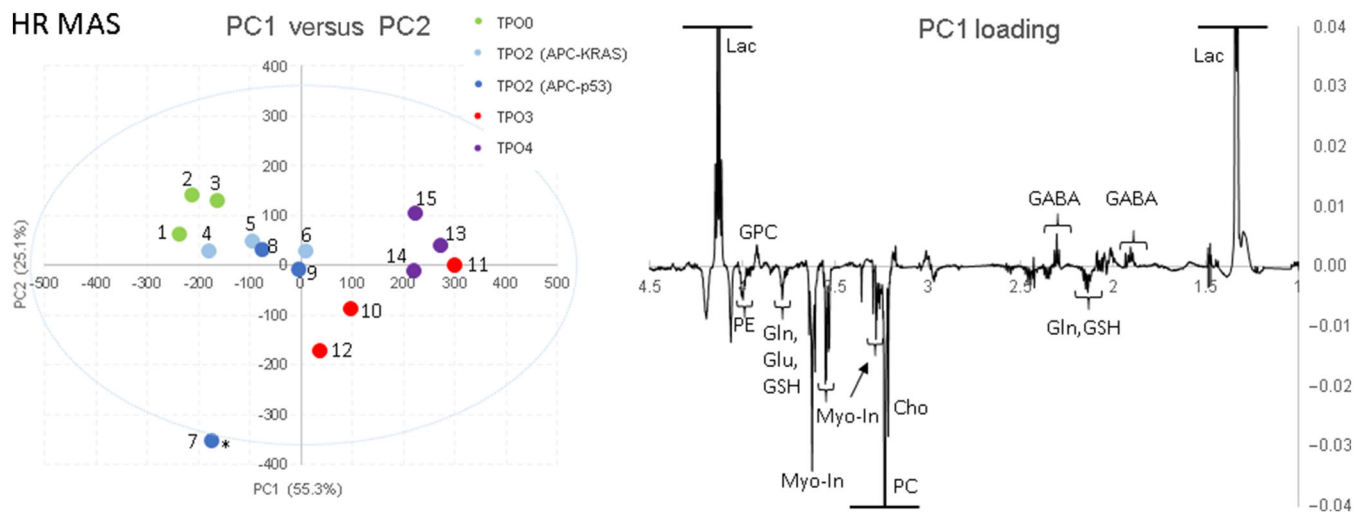


**FIGURE 6** PCA from HR MAS MRS. Left panel: PC1 versus PC2 score plot. Right panel: PC1 loading profiles. Quantified metabolites from the spectral region with poorer SNR are not included (outside 1 and 4.5 ppm). Sample ID: 1: TPO0\_0 h, 2: TPO0\_48 h, 3: TPO0\_96 h, 4: TPO2\_0 h, 5: TPO2\_48 h, 6: TPO2\_96 h, 7: TPO2\_p53APC\_0 h, 8: TPO2\_p53APC\_48 h, 9: TPO2\_p53APC\_96 h, 10: TPO3\_0 h, 11: TPO3\_48 h, 12: TPO3\_96 h, 13: TPO4\_0 h, 14: TPO3\_48 h, 15: TPO4\_96 h. Cho, choline; GABA, gamma-aminobutyric acid; Gln, glutamine; Glu, glutamate; GPC, glycerophosphocholine; GSH, glutathione; HR MAS MR, high-resolution magic angle spinning magnetic resonance; Lac, lactate; Myo-In, myo-inositol; PC, phosphocholine; PCA, principal component analysis; PE, phosphoethanolamine; SNR, signal-to-noise ratio; TPO, tumor progression organoid

inspection of the spectra indicated that the two methods provide spectra of similar quality. Assignment of peaks confirmed that the two methods produce similar spectra, as the same 16 metabolites were quantified in both datasets. This suggests that loss of metabolites because of low extraction efficiency (extraction NMR) or interaction with macromolecules (HR MAS MRS) is unlikely to cause major differences between the two methods. As expected, polar extraction eliminates lipophilic compounds from the samples, while HR MAS MRS spectra contained lipid signals because T2 filtering was not applied. Lipid signals may carry significant biological information related to the tumor microenvironment and treatment response.<sup>17,18</sup> However, we did not detect significant differences in the lipid profiles between any of the TPO types.

The similarity of the spectra obtained with HR MAS MRS and extraction NMR was further confirmed by the correlation analysis. As the total signal intensity of the spectra varied between the methods, we chose to normalize to the total area under the curve for the assigned metabolites. Similar indirect approaches for comparison of HR MAS MRS and extraction NMR have also been used by others.<sup>19</sup> The global correlation was good ( $R = 0.94$ ,  $p < 0.0001$ ), but was notably lower for some of the individual metabolites. Although this could be caused by variable extraction efficiency, the lowest correlations were found for metabolites that were difficult to integrate accurately due to low signal-to-noise ratio and/or poor spectral resolution. Importantly, the multivariate analysis clearly demonstrated that both HR MAS MRS and extraction NMR successfully differentiated the TPOs. The loading profiles were strikingly similar, identifying Lac, PC, and Myo-In as the major metabolites contributing to the differentiation. As PCA is an unsupervised method with high sensitivity for systematic differences in spectral information, these results indicate that HR MAS NMR and extraction NMR are functionally equivalent for metabolic analysis of organoids.<sup>14</sup>

While extraction NMR is potentially best suited for focused analysis of polar metabolites present in low concentrations, HR MAS MRS is performed after a minimum of sample preparation. This has several advantages, such as the absence of spectral contamination caused by components used in the extraction procedure and the nondestructive nature of the method in contrast to extraction NMR. Moreover, the organoids may be recovered after HR-MAS analysis to extract nucleic acids or isolate proteins.<sup>9</sup> HR MAS also provides a more direct link for translation to in vivo MRS, as the organoids are intact.

PCA indicated systematic associations between the metabolic profile of the organoid lines and their mutational profile. The TPO lines are designed to represent the typical sequential acquisition of specific genetic alterations that underlies the progression of colorectal cancer.<sup>10</sup> The relationship between the metabolic reprogramming frequently observed in cancer and the stepwise malignant transformation is poorly understood, but our data suggest a gradual drift towards the cancer-specific phenotype. Specifically, the Lac levels increase gradually with the number of mutations. All the mutations in the organoid lines have been suggested to contribute to deregulated glycolytic activity in cancer, and our data indicate that these metabolic effects of mutations are additive.<sup>20-22</sup>

The data also indicate that the Myo-In levels of the organoids decreased with the number of mutations. Myo-In is not universally recognized as a metabolic biomarker in cancer, but there is ample evidence that inositol metabolism is dysregulated in cancer.<sup>23,24</sup> Mechanistic studies of inositol metabolism in this TPO organoid model system could potentially contribute to an improved understanding of how this metabolic pathway is involved in cancer progression.

We observed a negative association between PC level and the number of mutations. The general consensus on Cho metabolism in cancer is that the level of PC increases with malignancy.<sup>25,26</sup>

However, several reports suggest differential regulation of Cho metabolism in vitro and in vivo.<sup>5,27</sup> Furthermore, metabolic profiling of colorectal biopsies has suggested that PC levels are higher in benign lesions than in both normal intestinal epithelium and colorectal cancer.<sup>28</sup> Because it has been suggested that PC levels correlate with the cellular proliferation rate,<sup>29</sup> the metabolic landscape in colorectal cancer may contrast to that of other cancers due to the high proliferation rate of intestinal epithelium in its natural state. Again, multicellular spheroids may represent a more relevant model for mechanistic studies of metabolism than cells cultured in monolayers.

## 5 | CONCLUSIONS

Overall, this study shows that the metabolic data obtained by HR MAS MRS analysis of intact organoids are highly similar to those obtained with polar extraction NMR. Both correlation analysis and PCA indicate that HR MAS MRS can be used in metabolic profiling of organoids and other 3D cell culture systems. In our setup, HR MAS MRS offered the advantage of minimal sample preparation and nondestructive analysis. The latter makes this technique closer in resemblance to in vivo MR spectroscopy. Finally, comparison of metabolic profiles from TPOs indicate that metabolic changes occur at a very early stage of disease progression. Successive accumulation of mutations was associated with a gradual alteration in metabolic characteristics.

## ACKNOWLEDGMENTS

Experiments at the 600 MHz instrument for solution NMR were supported by uNMR-NL, the National Roadmap Large-Scale NMR Facility of the Netherlands (NWO grant 184.032.207). The authors are indebted to I. Verlaan-Klink, M. L. Ludikhuizen, M. J. Rodriguez-Colman, and M. Meerlo for advice on organoid culturing and providing starting batches of the organoids. The HR MAS MRS analyses were performed at the MR Core Facility, Norwegian University of Science and Technology (NTNU). The MR core facility is funded by the Faculty of Medicine at NTNU and Central Norway Regional Health Authority.

## ORCID

Jeanine J. Prompers  <https://orcid.org/0000-0002-4756-4474>

Tone Frost Bathen  <https://orcid.org/0000-0002-8582-6965>

## REFERENCES

1. Munir R, Liseic J, Swinnen JV, Zaidi N. Too complex to fail? Targeting fatty acid metabolism for cancer therapy. *Prog Lipid Res.* 2021;85:101143. doi:10.1016/j.plipres.2021.101143
2. Chu QS, Sangha R, Spratlin J, et al. A phase I open-labeled, single-arm, dose-escalation, study of dichloroacetate (DCA) in patients with advanced solid tumors. *Invest New Drugs.* 2015;33(3):603-610. doi:10.1007/s10637-015-0221-y
3. Porper K, Shpatz Y, Plotkin L, et al. A phase I clinical trial of dose-escalated metabolic therapy combined with concomitant radiation therapy in high-grade glioma. *J Neurooncol.* 2021;153(3):487-496. doi:10.1007/s11060-021-03786-8
4. Harding JJ, Telli M, Munster P, et al. A phase I dose-escalation and expansion study of telaglenastat in patients with advanced or metastatic solid tumors. *Clin Cancer Res.* 2021;27(18):4994-5003. doi:10.1158/1078-0432.CCR-21-1204
5. Mori N, Wildes F, Takagi T, Glunde K, Bhujwala ZM. The tumor microenvironment modulates choline and lipid metabolism. *Front Oncol.* 2016;6:262. doi:10.3389/fonc.2016.00262
6. Drost J, Clevers H. Organoids in cancer research. *Nat Rev Cancer.* 2018;18(7):407-418. doi:10.1038/s41568-018-0007-6
7. Sachs N, Clevers H. Organoid cultures for the analysis of cancer phenotypes. *Curr Opin Genet Dev.* 2014;24:68-73. doi:10.1016/j.gde.2013.11.012
8. Sato T, Vries RG, Snippert HJ, et al. Single Lgr5 stem cells build crypt-villus structures in vitro without a mesenchymal niche. *Nature.* 2009;459(7244):262-265. doi:10.1038/nature07935
9. Moestue S, Sitter B, Bathen TF, Tessem MB, Gribbestad IS. HR MAS MR spectroscopy in metabolic characterization of cancer. *Curr Top Med Chem.* 2011;11(1):2-26. doi:10.2174/156802611793611869
10. Mori N, van Jaarsveld RH, Ponsioen B, et al. Sequential cancer mutations in cultured human intestinal stem cells. *Nature.* 2015;521:43-47. doi:10.1038/nature14415
11. Watanabe K, Ueno M, Kamiya D, et al. A ROCK inhibitor permits survival of dissociated human embryonic stem cells. *Nat Biotechnol.* 2007;25(6):681-686. doi:10.1038/nbt1310
12. Eilers PH. Parametric time warping. *Anal Chem.* 2004;76(2):404-411. doi:10.1021/ac034800e
13. Savorani F, Tomasi G, Engelsen SB. icoshift: A versatile tool for the rapid alignment of 1D NMR spectra. *J Magn Reson.* 2010;202(2):190-202. doi:10.1016/j.jmr.2009.11.012
14. Debik J, Sangermani M, Wang F, Madssen TS, Giskeødegård GF. Multivariate analysis of NMR-based metabolomic data. *NMR Biomed.* 2021;35:e4638. doi:10.1002/nbm.4638
15. Giskeødegård GF, Madssen TS, Euceda LR, Tessem MB, Moestue SA, Bathen TF. NMR-based metabolomics of biofluids in cancer. *NMR Biomed.* 2018;32:e3927. doi:10.1002/nbm.3927

16. Nagana Gowda GA, Raftery D. Can NMR solve some significant challenges in metabolomics? *J Magn Reson*. 2015;260:144-160. doi:[10.1016/j.jmr.2015.07.014](https://doi.org/10.1016/j.jmr.2015.07.014)
17. Arlauckas SP, Browning EA, Poptani H, Delikatny EJ. Imaging of cancer lipid metabolism in response to therapy. *NMR Biomed*. 2019;32(10):e4070. doi:[10.1002/nbm.4070](https://doi.org/10.1002/nbm.4070)
18. Delikatny EJ, Chawla S, Leung DJ, Poptani H. MR-visible lipids and the tumor microenvironment. *NMR Biomed*. 2011;24(6):592-611. doi:[10.1002/nbm.1661](https://doi.org/10.1002/nbm.1661)
19. Ratai EM, Pilkenton S, Lentz MR, et al. Comparisons of brain metabolites observed by HRMAS 1H NMR of intact tissue and solution 1H NMR of tissue extracts in SIV-infected macaques. *NMR Biomed*. 2005;18(4):242-251. doi:[10.1002/nbm.953](https://doi.org/10.1002/nbm.953)
20. Cha PH, Hwang JH, Kwak DK, Koh E, Kim KS, Choi KY. APC loss induces Warburg effect via increased PKM2 transcription in colorectal cancer. *Br J Cancer*. 2021;124(3):634-644. doi:[10.1038/s41416-020-01118-7](https://doi.org/10.1038/s41416-020-01118-7)
21. Hutton JE, Wang X, Zimmerman LJ, et al. Oncogenic KRAS and BRAF drive metabolic reprogramming in colorectal cancer. *Mol Cell Proteom*. 2016;15(9):2924-2938. doi:[10.1074/mcp.M116.058925](https://doi.org/10.1074/mcp.M116.058925)
22. Papageorgis P, Cheng K, Ozturk S, et al. Smad4 inactivation promotes malignancy and drug resistance of colon cancer. *Cancer Res*. 2011;71(3):998-1008. doi:[10.1158/0008-5472.CAN-09-3269](https://doi.org/10.1158/0008-5472.CAN-09-3269)
23. Benjamin DI, Louie SM, Mulvihill MM, et al. Inositol phosphate recycling regulates glycolytic and lipid metabolism that drives cancer aggressiveness. *ACS Chem Biol*. 2014;9(6):1340-1350. doi:[10.1021/cb5001907](https://doi.org/10.1021/cb5001907)
24. Ren L, Hong ES, Mendoza A, et al. Metabolomics uncovers a link between inositol metabolism and osteosarcoma metastasis. *Oncotarget*. 2017;8(24):38541-38553. doi:[10.18632/oncotarget.15872](https://doi.org/10.18632/oncotarget.15872)
25. Aboagye EO, Bhujwala ZM. Malignant transformation alters membrane choline phospholipid metabolism of human mammary epithelial cells. *Cancer Res*. 1999;59(1):80-84.
26. Glunde K, Bhujwala ZM, Ronen SM. Choline metabolism in malignant transformation. *Nat Rev Cancer*. 2011;11(12):835-848. doi:[10.1038/nrc3162](https://doi.org/10.1038/nrc3162)
27. Moestue SA, Borgan E, Huuse EM, et al. Distinct choline metabolic profiles are associated with differences in gene expression for basal-like and luminal-like breast cancer xenograft models. *BMC Cancer*. 2010;10:433. doi:[10.1186/1471-2407-10-433](https://doi.org/10.1186/1471-2407-10-433)
28. Tessem MB, Selnaes KM, Sjurset W, et al. Discrimination of patients with microsatellite instability colon cancer using 1H HR MAS MR spectroscopy and chemometric analysis. *J Proteome Res*. 2010;9(7):3664-3670. doi:[10.1021/pr100176g](https://doi.org/10.1021/pr100176g)
29. Podo F. Tumour phospholipid metabolism. *NMR Biomed*. 1999;12(7):413-439. doi:[10.1002/\(SICI\)1099-1492\(199911\)12:73.O.CO;2-U](https://doi.org/10.1002/(SICI)1099-1492(199911)12:73.O.CO;2-U)

**How to cite this article:** van der Kemp WJM, Grinde MT, Malvik JO, et al. Metabolic profiling of colorectal cancer organoids: A comparison between high-resolution magic angle spinning magnetic resonance spectroscopy and solution nuclear magnetic resonance spectroscopy of polar extracts. *NMR in Biomedicine*. 2022;e4882. doi:[10.1002/nbm.4882](https://doi.org/10.1002/nbm.4882)